ON THE PREDICTION OF BORON DILUTION USING THE CMFD CODE TRANSAT: THE ROCOM TEST CASE

M. Labois[1], J. Panyasantisuk[1], T. Höhne[2], S. Kliem[2], D. Lakehal[1]

[1]*ASCOMP GmbH*
Technoparkstrasse 1, CH-8005 Zurich, Switzerland

[2]*Forschungszentrum Rossendorf, Institute of Safety Research (FZD)*
P.O. Box 510119, 01314 Dresden, Germany

Abstract

This contribution aims at introducing a new multiscale, multicomponent CFD/CMFD approach for the simulation of thermal-hydraulics flows evolving in complex component-scale configurations. In this novel approach, the flow system could involve one or two fluids, convective and conductive heat transfer in solids, and phase-change heat transfer. This is made possible thanks to the Immersed Surfaces Technology (IST), a methods inspired from Interface Tracking techniques for two-phase flow, whereby solid bodies contained in the system are defined using a solid level set function to describe their surfaces, transcending conventional unstructured and body-fitted grids (BFC). In a typical two-phase flow, material properties of the fluids and the solid are segregated based on the gas-liquid and solid Level-Set functions. The technique helps solve conjugate heat transfer problems without resorting to explicit jump conditions. Selected validation test-cases are presented here. The main application includes steady and transient solutions of the boron dilution in the ROCOM test case.

1. INTRODUCTION

Computational thermal hydraulics – by reference to mesoscale or component scale (see Yadigaroglu & Lakehal, 2005) - has been facing the same set-up problems encountered in many other engineering applications that resort to CFD (e.g. aerodynamics, turbomachinery, etc.), namely dealing with complex configurations in terms of grid generation. The task is known to require sometimes up to 70% time of the entire simulation process. Although unstructured grids have somewhat helped invert the tendency, these techniques still need to be coupled with structured body-fitted coordinate (BFC) meshes in the boundary layer. The IST method of TransAT has solved the grid generation problem in this area, whereby all sorts of geometries are mapped into a Cartesian grid. IST helps solve the problem in a convenient way, using a Cartesian structured grid in which solid bodies are described using the level set technique borrowed from two-phase flow modelling (using Interface Tracking Methods –ITM-; see Lakehal et al, 2002). These approaches are shown to be applicable to different turbulence modelling approaches, including standard $k-\varepsilon$ model and LES. The IST approach will be presented in the first part of this paper, without details of the model implementation, together with the BMR technique, short for Block Mesh Refinement. This was developed in TransAT to help better solve the boundary layer zone when use is made of IST. In BMR, more refined sub-blocks can be automatically generated around solid surfaces; with dimensions made dependent on the Reynolds or Grashoff number. The associated applications will be presented in the second part of the paper, including flow past a circular cylinder. The main application to be discussed includes the steady and transient solution of the boron dilution in the ROCOM test case introduced next.

2. FLOW MIXING FOR SAFETY ANALYSIS

Within nuclear reactor safety analyses, one of the events that could potentially lead to a criticality accident is a small break loss of coolant accident (LOCA) inducing a dilution in the steam generators tubes by reflux condensation followed by the restart of the natural circulation (Rohde et al, 2008). In the event of a LOCA, density differences between the coolant water and the primary loop inventory

play an important role, as the injection of cold emergency core cooling (ECC) water induces thermal stratification increasing thermal stresses on the RPV walls (Bieder & Graffard, 2008). This situation can only be mitigated by the mixing at the core inlet, where partial mixing takes place. In pressurized water reactors (PWR), boric acid is used as a neutron absorber for reactivity control. If the boric acid concentration in the core region is reduced, a power excursion with possible fuel damage might occur.

Figure 1: The ROCOM vessel model (from FZD).

Mixing is a direct consequence of a complex three-dimensional fluid flow, which itself depends on the concentration of the additives (Höhne et al., 2006). Detailed mixing pattern at the core inlet is required to make accurate and realistic predictions about the safety of the reactors, a task that is today within reach of state-of-the-art CFD. Indeed, Höhne et al. (2006) used both CFX-5 and Trio-U for the same problem in steady state. Schaffrath et al. (2007) employed the CFD code FLUENT, in steady-state and transient conditions. Höhne et al. (2008) report new transient results (U-RANS), also using ANSYS CFX. Various measurement campaigns were performed worldwide to understand the phenomena associated with boron dilution in PWRs. The Rossendorf Coolant Mixing Model (ROCOM) operated by FZD is one of these (Prasser et al., 2003; Höhne et al., 2006, 2008. The transparent 1:5 linear scaled test facility shown in Fig. 1 simulates German PWRs and includes all important details for coolant mixing. It has four loops each equipped with an individually controlled pump to enable the performance of tests in a wide range of flow conditions: ranging from natural convection flow-up to forced convection flow at nominal flow rates, including flow ramps (e.g., due to pump start-up). ROCOM is operated with water at ambient temperatures as the reactor RPV mock-up and its internals are made of Perspex. The designers paid special attention to all components which significantly influence the velocity fields: the core barrel with the lower support plate and the core simulator, the perforated drum in the lower plenum, and the inlet and outlet nozzles of the main coolant lines with diffuser elements. For the investigation of boron dilution transients, disturbances are created by computer-controlled injection of a tracer (salt water solution) into the cold leg of one or two of the loops near the inlet nozzle. The facility was equipped with fast-acting pneumatic gate valves (opening time 3 s) to cut-off the part of the loops where disturbances are generated. The initial test conditions were checked by a wire mesh sensor at the RPV mock-up inlet nozzles. Since the boron content influences the fluid density, this was adjusted by adding ethyl alcohol.

2. THE MULTISCALE, MULTICOMPONENT APPROACH

2.1. The Physical Model

In TransAT, the RANS equations for incompressible single-fluid flow and convective heat transfer are formulated in the following conservative form:

$$\frac{\partial \rho}{\partial t}+\frac{\partial}{\partial x_j}\left(\rho \bar{u}_j\right)=0$$

$$\frac{\partial\left(\rho \bar{u}_i\right)}{\partial t}+\frac{\partial\left(\rho \bar{u}_i \bar{u}_j\right)}{\partial x_j}=-\frac{\partial \bar{p}}{\partial x_i}+2\mu\frac{\partial \bar{S}_{ij}}{\partial x_j}-\frac{\partial \tau_{ij}}{\partial x_j}+F_b \qquad (1)$$

$$\frac{\partial\left(\rho Cp\bar{T}\right)}{\partial t}+\frac{\partial\left(\rho Cp\overline{\bar{T}\bar{u}_j}\right)}{\partial x_j}=\lambda\frac{\partial \bar{T}}{\partial x_j}-\frac{\partial q_t^{\cdot}}{\partial x_j}+Q'''$$

where **u** stands for the fluid velocity and P for the pressure, ρ is the density, μ is the viscosity, is the thermal conductivity, S_{ij} is the rate of deformation tensor, and Q''' is the volumetric heat source. The third term in the RHS of the momentum equation (F_b) represents body forces, e.g. to account for buoyancy effects due to temperature variations. The Reynolds stress tensor τ and the turbulent scalar flux q_t are modelled using the eddy viscosity concept, i.e. within the $k-\varepsilon$ model. The turbulent kinetic energy and rate of dissipation k and ε equations are solved taking into account the effect of buoyancy-induced production/dissipation.

2.2. The IST/BMR Approach

The IST was developed by ASCOMP, and differs slightly from the Immersed Boundary Methods (see for review, Mittal & Iaccarino, 2005), albeit the methods share the same principle of immersing solid objects within a Cartesian grid. The idea is to represent solid walls by a Level Set function representing the exact distance to the surface, which is zero at the surface, positive in the fluid and negative in the solid (c.f. Fig. 2). The fluid and the solid have their own material properties, based on the Level Set function: density, heat capacity and thermal conductivity. The technique has the major advantage to solve conjugate heat transfer problems, in that conduction inside bodies is directly linked to external fluid convection. In practice, the CAD file of the solid is immersed into a cubical grid covered by a Cartesian mesh, but the Navier-Stokes equations are modified to account for the presence of the solid Level-Set function. The treatment of wall shear is handled differently though, as explained below. Compared to Peskin's (1972) 1st-order method, IST is second order near the walls.

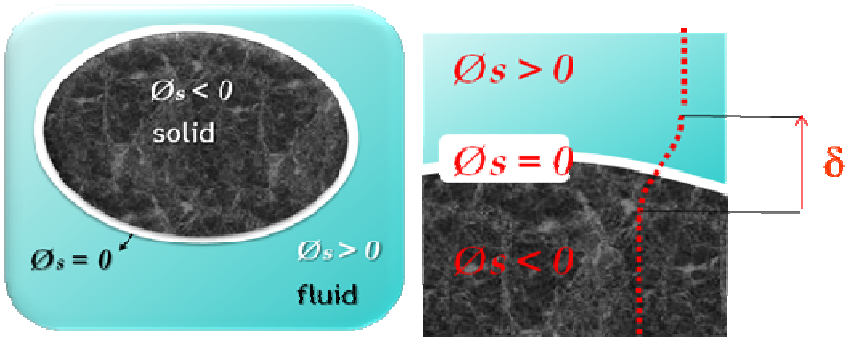

Figure 2: Representation of materials using IST. The right panel shows the smooth wall layer.

The BMR technique was developed in TransAT to help better solve the boundary layer zone when use is made of the IST technique discussed above. In BMR, more refined sub-blocks can be automatically generated around solid surfaces; with dimensions made dependent on the Reynolds number (the sub-block scale should always be set such that it covers the boundary layer thickness), or the first wall-cell is determined based on the turbulence model to be used; e.g. Wall Functions or Two-Layer model for both smooth and rough walls. Sub-blocks of different refinement can be generated, with connectivity between the blocks matching up to 1-to-8 cells.

2.3. The Multicomponent Formulation

The immersed surface is represented on the Eulerian grid by a solid Level-Set function denoted by ϕ_s that is a signed distance function, which is positive in the solid domain, is negative in the fluid phase, and is zero at the fluid–solid frontier. The equations in the solid and fluid domain are combined using a smooth Heaviside function which takes value 1 in the fluid phase and 0 in the solid domain:

$$H(\phi_s) = \left[1 - \tanh\left(2\phi_s / \delta_{sf}\right)\right] / 2 \tag{2}$$

where δ_{sf} is the solid–fluid finite interface thickness. In the multicomponent formulation implemented in TransAT, the momentum equations for the fluid phase are reformulated as follows:

$$\frac{\partial\left(\rho\overline{u_i}\right)^f}{\partial t} + \frac{\partial\left(\rho\overline{u_i}\,\overline{u_j}\right)^f}{\partial x_j} = -H(\Phi_s)\frac{\partial\overline{p^f}}{\partial x_i} + 2\mu\frac{\partial\overline{S_{ij}^f}}{\partial x_j} - \frac{\partial\tau_{ij}^f}{\partial x_j} - F_w + F_s + F_b \tag{3}$$

where the additional source terms in Eq. (3) denote the viscous shear at the wall (F_w) and the surface tension between the fluid phases (F_s) formulated within the level set approach of Sussman et al. (1994). The wall shear itself is modelled as:

$$2\mu_i^f\overline{S_{ij}^f}n_j\delta(\Phi_s) \equiv 2\left(\frac{\rho^s}{\rho^f}\right)\frac{\overline{U_w}}{H(\Phi_s)}\delta(\Phi_s) \tag{4}$$

where **n** is the normal to the fluid–solid interface, U_w is the fluid velocity parallel to the wall, and $\delta(\phi_s)$ is the Dirac delta function representing the location of the wall surface. Material properties including density, viscosity, thermal conductivity, heat capacity depend locally on the gas-liquid and fluid-solid level set functions, ϕ and ϕ_s. The well-known turbulence scalar ($k-\varepsilon$) equations are also slightly modified to account for immersed solids. When used in combination with RANS turbulence modelling with wall-functions, the wall shear is calculated using the logarithmic law of the wall, and is incorporated as a retarding wall-adjacent force in the momentum equations. Since the walls are immersed in a Cartesian grid, meshing time is considerably reduced and the accuracy of the numerical scheme can be preserved since the grid-skewness induced diffusion is simply eliminated. These advantages are particularly desirable for LES and ITM schemes (e.g. VOF and Level Sets), which are not very satisfactory when use is made of BFC and unstructured grids; in both LES and ITM the results are very sensitive to grid quality. These elements make the IST/BMR approach very useful to simulate unsteady turbulent single and multicomponent flows evolving in complex geometries.

2.4. The Numerical Approach

The CMFD code TransAT© of ASCOMP is a multi-physics, finite-volume code based on solving multi-fluid Navier-Stokes equations. The code uses structured meshes, though allowing for multiple blocks to be set together. MPI parallel based algorithm is used in connection with multi-blocking. The grid arrangement is collocated and can thus handle more easily curvilinear skewed grids. The solver is pressure based (Projection Type), corrected using the Karki and Patankar (1989) technique for subsonic-to-transonic compressible flows (M < 2). High-order time marching and convection schemes can be employed; up to third order Monotone schemes in space (Quick scheme of Leonard), and 3rd to 5th order Runge-Kutta schemes for time marching. Turbulent flows can be tackled within both the RANS and LES and its variant V-LES (short for Very Large Eddy Simulation). Multiphase flows can be tackled using (1) interface tracking techniques for both laminar and turbulent flows (level set, VOF with CVTNA interface reconstruction, and Phase Field), (2) phase-averaged homogeneous model (Algebraic Slip), and (3) Lagrangian particle tracking (1-to-4 way coupling, with heat transfer).

3. VALIDATION EXERCISES

3.1. Laminar Flow past a Circular Cylinder

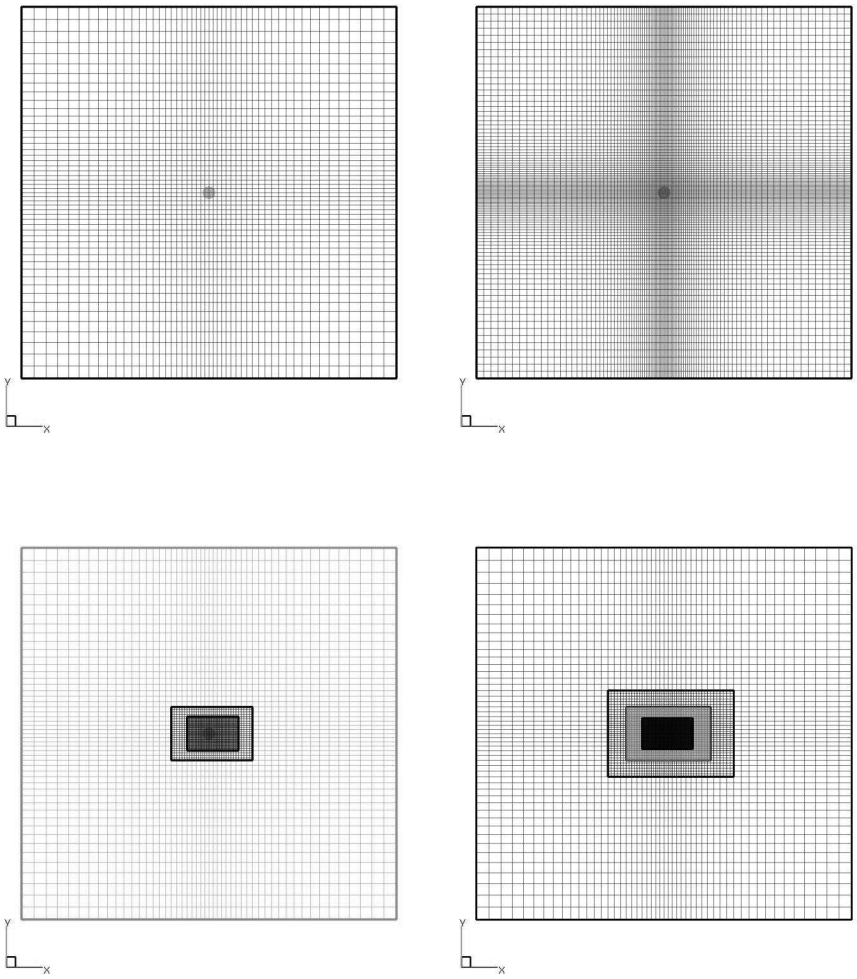

Figure 2: Meshing techniques used for the flow past a cylinder: body-fitted grid, IST and IST/BMR

This first validation test-case consists in the laminar flow past a circular cylinder at Re = 20-100, based on cylinder diameter and inflow velocity. Steady and unsteady simulations were performed using body-fitted grids (BFC) as the reference case, and Cartesian grids within the IST context, with and without BMR manifolds refinements. For all these simulations, a grid independence study has been performed, with mesh sizes ranging between 25'000 and 40'000 cells to address the gridding effect with IST/BMR. The different types of mesh used are presented in Fig. 3; the first panels show the single-block IST grids (medium and fine) with no additional BMR manifolds; the second panels show the IST grids with 3 and 4 BMR levels, respectively. The simulation result discussed here is the flow at Re = 40. Pressure and velocity fields of the fine-grid BFC and 4-level IST/BMR solutions at steady state are compared in Fig. 4. The comparison shows that the two approaches deliver identical results. Further validation results are discussed in Table 1, summarizing the predicted Drag coefficients obtained with the different approaches: BFC (from coarse to very fine); IST (1 BMR level, from coarse to very fine), and IST/BMR (from 2 to 4 levels BMR sub-blocks).

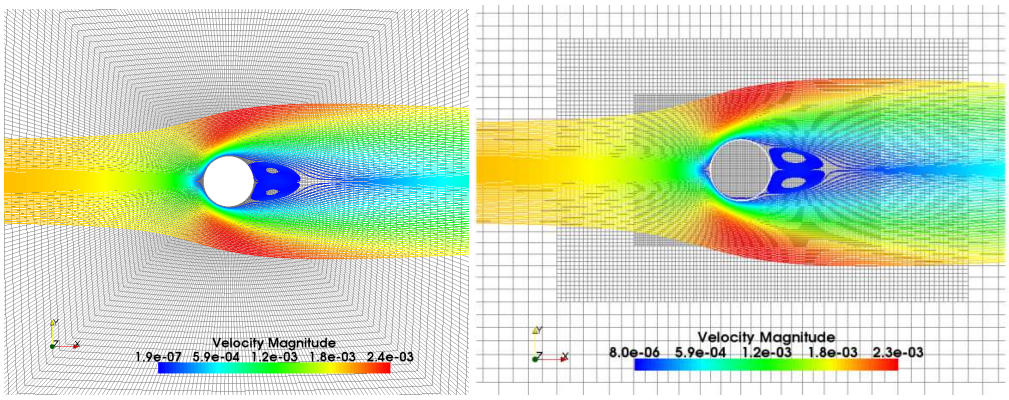

Figure 4: Flow past a cylinder (Re=40): pressure field and streamlines for BFC (left) and IST/BMR (right).

Grid	Description	No of cells	Grid efficiency	C_D
1	Base Grid	2500	6.25%	1.71300
2	Fine Grid	10000	25.00%	2.12050
3	Very fine grid	40000	1000.00%	2.09636
4	2-level BMR grid	2756	6.89%	2.24825
5	3-level BMR grid	4788	11.97%	2.13764
6	4-level BMR grid	23756	59.39%	2.09909
7	Coarse body-fitted grid	2500	6.25%	2.04300
8	Fine body-fitted grid	40000	100.00%	2.08700

Table1: Drag coefficients obtained with different meshing techniques and different grid refinements.

The simulation on the finest BFC grid (40'000 nodes) is taken as the reference solution, delivering a drag coefficient of C_D = 2.087. From these results it can be seen that if the mesh is not too coarse, IST provides results which are in excellent agreement with reference results. Looking now at the IST/BMR results reveals that results are also in very good agreement with the BFC mesh, while the number of cells has sharply decreased: when using three levels of refinement, more than 40% of the number of cells is saved to obtain results with the same quality; CD = 2.099, equivalent to the finest IST results (CD = 2.096). The conclusions to be drawn here are: (1) single-block IST deliver similar results as BFC (the advantage here is rapid gridding) for the same grid resolution, and (2) multi-block IST/BMR deliver the same results as BFC, for the same grid resolution near the boundary layer, but overall saving up to 40% cells in 2D; about 75% in 3D depending on the test cases.

For flow past the cylinder at Re = 100, the motion is now unsteady featuring vortex shedding. Thus, the Strouhal number (St) could be compared to values found in the literature. The St obtained with the Grid-3 simulation is St = 0.166, which compares very well to previous experimental results of Williamson (St = 0.166) and Roshko (St = 0.167); both reported by Lai and Peskin (2000). Lai and Peskin (2000), who performed a similar calculation using immersed boundaries found St = 0.13-0.165. The results obtained with IST/BMR are in excellent agreement with the data.

4. BORON CONCENTRATION PREDICTION: THE ROCOM TEST CASE

4.1. Simulation Parameters

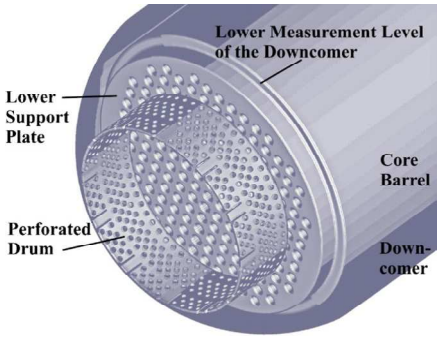

Figure 5: The original ROCOM CAD file (details of the drum).

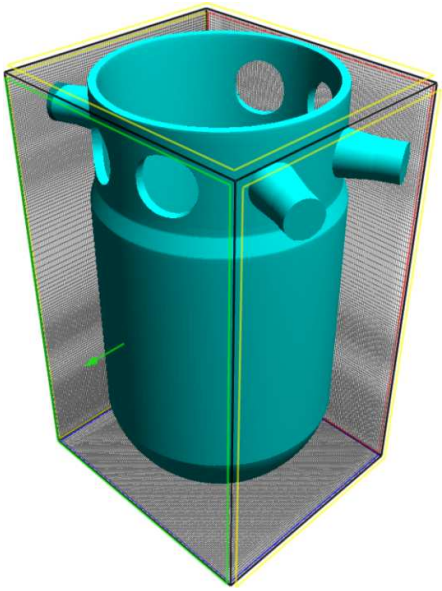

Figure 6: IST-based grid for the ROCOM problem.

Steady state and transient flow simulations were performed by TransAT using the $k-\varepsilon$ model for turbulence, combined with wall functions. The model employed is as described in Eq. (3), in the single-phase formulation, where $F_s = 0$. The high-order convection scheme (Quick) of Leonard was employed for all variables. The CAD files shown in Fig. 5 including the details of the drum (right) were immersed in a Cartesian grid consisting of 2.15 million cells (Fig. 6); the fine grid used for comparison consists in 4.47 million cells. The analyzed experiment is characterized as density dominated (Froude number = 0.366). For this calculation, the main pump no. 1 is delivering 5% of the nominal mass flowrate. The density difference between the injected ECC water and the primary loop coolant is 10%. The other pumps are not working. Inlet boundary conditions were specified at the ECC injection line using uniform velocities to simulate the one-loop Operation. An outflow condition was specified at the outlet nozzles. A no-slip boundary condition with all functions was used at all solid walls. The IST method was applied. OpenMP parallel steady-state computation took 8h on 4-CPU PC cluster operating under Linux; transient runs took 72H. The simplifications brought to the original geometry by the FZR group (Höhne et al., 2006) were maintained here, too.

4.2. Steady State Results

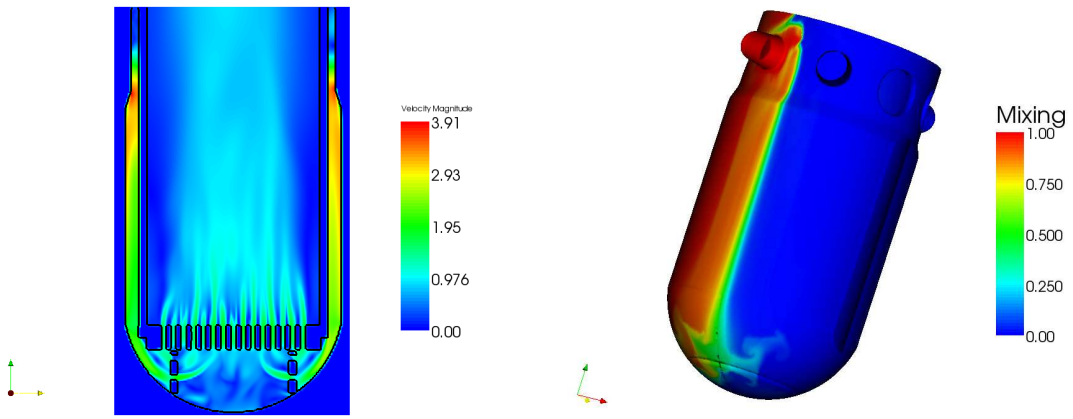

Figure 7: Flow and scalar mixing obtained by TransAT.

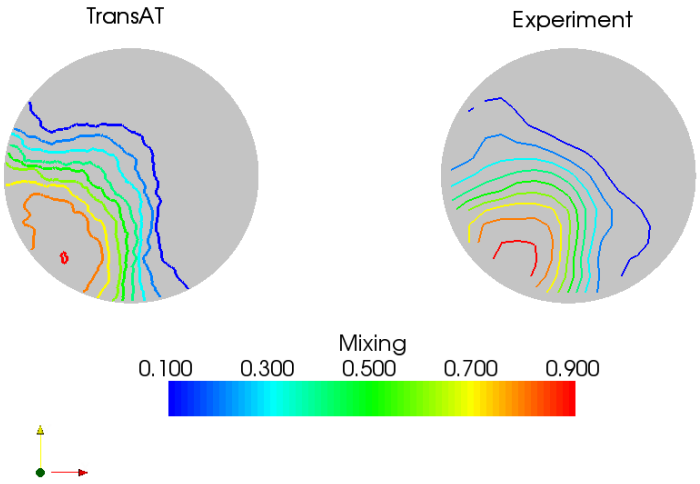

Figure 8: Measured vs. simulated boron mixing in a cross section above the perforated drum.

The CFD results are discussed in the context of Figs. 7 and 8. The left panel of Fig. 7 displays the velocity iso-contours, showing the details of the flow captured by the method without use of the porosity approach. The flow penetrates deep into the vessel then raises upward through the perforated drum. The right panel displays the boron distribution along the downcomer internals. Figure 8 compare experimental and CFD results of the scalar mixture at a flow cross-section located just above the perforated drum. The simulation results agree pretty well with the data of Rohde et al. (2005), although the maximum concentration is underestimated compared to the data (red contour-lines). This was to be expected from isotropic eddy viscosity model, which are known to underestimate the rate of spreading of scalars near the walls, where turbulent stresses and fluxes are actually highly anisotropic.

4.3. Transient Results

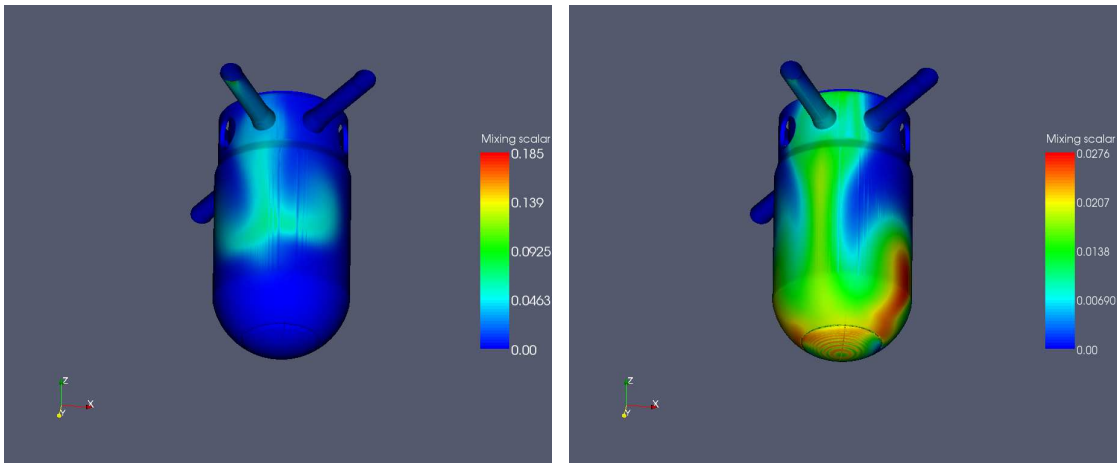

Figure 9: Transients of Boron distribution in the vessel.

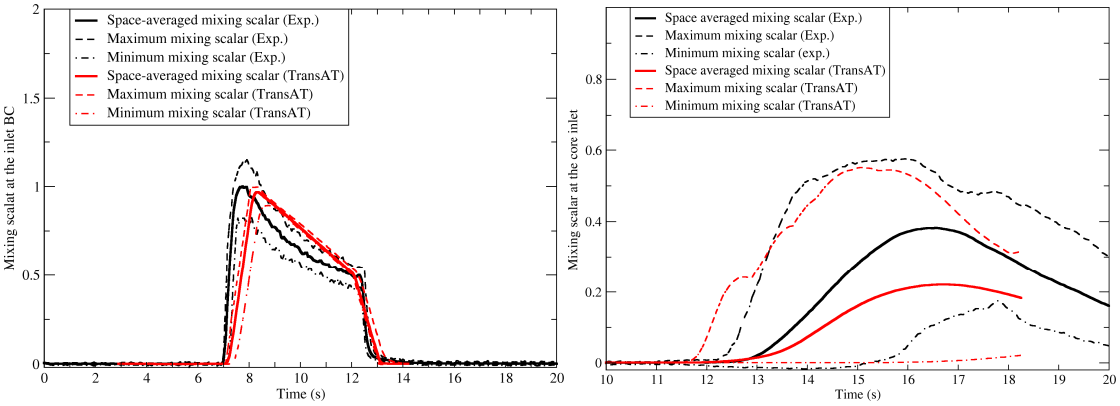

Figure 10: Measured vs. simulated scalar concentration at inlet at core inlet.

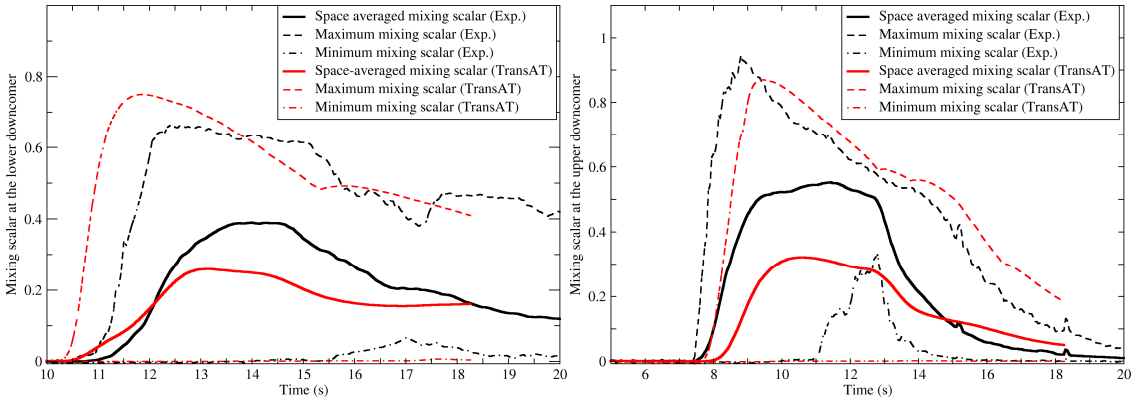

Figure 11: Measured vs. simulated boron mixing scalar concentration at inlet at lower and upper downcomer.

In the transient simulation, the flow is initiated at one pipe only. The simulation conditions considered here are widely inspired from the paper of Höhne et al., (2008) dealing with transients in this flow.

The same computational parameters are employed as in the steady-state case discussed previously, except that here the pipe length is substantially larger now to ensure developed flow conditions be reached before the flow enters the core inlet. A second-order implicit time marching scheme is employed. A U-RANS approach is employed, with an adaptive time step oscillating around a mean value of 0.001s, controlled via both convective and diffusive CFL criteria bounded between 1 and 2. The simulations run for 20s before reaching pseudo steady-state conditions.

Qualitative results of the transient simulation are discussed in the context of Fig. 9, depicting the tracer concentration with time. Figures 10 and 11 present the history of the maximum, average and minimum tracer concentrations at selected locations. The left panel of Fig. 9 depicts the early stage of tracer penetration, suggesting that the scalar behaves like a vertical jet with little lateral/radial spreading around the vessel internals. The behaviour is more visible in the right panel, showing a later-stage snapshot of the scalar. At the pipe inlet, the scalar concentrations (maximum, minimum and maximum) are in line with the data; at the core inlet, however, deviations between CFD and experiments are visible when looking at the minimum values in particular, and thus the space averaged value. The maximum values are in accordance though. This is due to the fact that the pipe is not long enough to allow the flow and scalar concentration to reach fully developed conditions. At the lower and upper downcomer locations, again, the maximum concentration values match, but not the minimum values, and the thus the space averaged values. This could be interpreted by a low or slow lateral/circumferential spreading of the tracer along the internals. The reasons could be either numerical or physical (turbulence), or both: from the numerical viewpoint, it is likely that the grid is not fine enough to capture this distribution; while in terms of modelling, eddy viscosity models should systematically fail to predict momentum and scalar diffusion neighbouring the walls, because of the anisotropy of the stresses and fluxes. While the various papers from the FZR group report mainly space averaged distributions of the tracer, with no clear indication concerning the maxima and minima. Schaffrath et al. (2007) who employed the CFD code FLUENT for the same problem report comparison of the experimental and computational history of the maximum, space average and minimum tracer concentrations at the same locations (inlet, core inlet, lower and upper downcomer) showing similar deficiencies as observed here with TransAT.

5. CONCLUDING REMARKS

This paper describes a new multiscale, multicomponent CFD/CMFD approach for the simulation of single and multiphase thermal-hydraulics flows evolving in complex component-scale (mesoscale) configurations. In this approach the flow system could involve one or more fluids, convective and conductive heat transfer in solids, and phase-change heat transfer. The approach is based on the so-called Immersed Surfaces Technology (IST), whereby solid bodies contained in the system are defined using a solid level set function to describe their surfaces, transcending conventional unstructured and body-fitted grids (BFC). The method has been successfully employed to treat the Boron distribution in the complex ROCOM configuration, both under steady-state and transient conditions. The quality of the present simulations is comparable to TRIO-U, CFX and FLUENT results reported by Höhne et al. (2006, 2008) and Bieder and Graffard (2008).

Overall the quality of TransAT simulations pleads in favour of this multiscale, multicomponent approach based on IST/BMR. The method can now be can be faithfully used for a variety of thermal-hydraulics mixing problems with a major advantage that it generates realistic transient simulations of turbulent single and multiphase flows in reasonable computing times (of the order of 24H on PC Linux clusters), since it reduce the grid size and thus the simulation time. The method is now widely used in TransAT for other types of flows, using other modelling frameworks, including LES and V-LES. It has recently been successfully used to predict single phase flow and temperature mixing in a 128-tube steam generator, the results of which will be presented as well.

Acknowledgements

The simulations shown here were conducted using the TransAT code of ASCOMP by Daniel Caviezel and Dr Mathieu Labois, partially within the NURISP project funded by the EU Euratom project. The FZR group (Dr Ulrich Rohde, Dr. Dirk Lucas and Dr. Thomas Höhne) is gratefully acknowledged for having provided the ROCOM CAD files and measurement data.

REFERENCES

U. Bieder, E. Graffard, Qualification of the CFD code Trio-U for full scale reactor applications, Nuclear Eng. Design 238 (2008) 671–679

U. Bieder, E. Graffard, "Qualification of the CFD code Trio-U for full scale reactor applications", Nucl. Eng. Design, 238, 671–679, 2008.

T. Höhne, S. Kliem, U. Bieder, "Numerical modelling of a buoyancy driven flow experiment at the ROCOM test facility using CFD codes CFX & Trio U.", Nucl. Eng. Design, 236, 1309–1325, 2006.

T. Höhne, S., Kliem, U., Rohde, F.-P., Weiss, "Boron dilution transients during natural circulation flow in PWR—Experiments and CFD simulations",Nuclear Eng. & Design, 238, 1987–1995, 2008.

K.C. Karki, S.V. Patankar, "Pressure Based Calculation Procedure for Viscous Flows at All Speeds in Arbitrary Configurations", AIAA Journal 27, 1167-1174, (1989).

M.C. Lai, C.S. Peskin, "An Immersed Boundary Method with Formal Second-Order Accuracy and Reduced Numerical". JCP, 160(2), 705-719, (2000).

D. Lakehal, M. Meier, M. Fulgosi, "Interface Tracking towards the Direct Simulation of Heat and Mass Transfer in Multiphase Flows," Int. J. Heat & Fluid Flow, 23, 242-257, 2002.

R. Mittal, G. Iaccarino, "Immersed Boundary Methods", Ann. Rev. Fluid Mech, 37, 239–261, 2005.

H.-M. Prasser, G. Grunwald, T. Höhne, S. Kliem, U. Rohde, F.-P. Weiss, "Coolant mixing in a pressurised water reactor: deboration transients, steam-line breaks, and emergency core cooling injection". Nucl. Technol., 143, 37–56, 2003.

U. Rohde, S. Kliem, T. Höhne, R. Karlsson, B. Hemstrom, J. Lillingtonc, T. Toppilad, J. Eltere, Y. Bezrukov, "Fluid mixing and flow distribution in the reactor circuit", Nucl. Eng. Design, 235, 421–443, 2005.

C.S. Peskin, "Flow Patterns around Heart Valves - Numerical Method", JCP, 10, 252-271, (1972).

A. Schaffrath, K-Ch. Fischer, T. Hahm, S. Wussow, "Validation of the CFD code fluent by post-test calculation of a density-driven ROCOM experiment", Nuclear Eng. & Design, 237, 1899–1908, 2007,

S. Sussman, P. Smereka, S. Osher, "A Level set Approach for computing incompressible two-phase flow", J. Comp. Physics, 114, 146-161, 1994.

G. Yadigaroglu, D. Lakehal, "New trends in computational thermal hydraulics", Nuclear Technology, 152 (2), 239-251, 2005.